

Supplemental Information for Geospatial analysis of Alaskan lakes indicates wetland fraction and surface water area are useful predictors of methane ebullition

Contents

1. Supplementary Tables
2. Supplementary Figures
3. Citations

1. Supplementary Tables

Table SI1. Compiled regression results from past ebullition regression studies.

Reference	Model	R ²	Adj. R	rmse	aic	f	n	P<0.005?
Bastviken et al. 2004	log(Area)		0.78				17	yes
	log(Area) + log(TP)		0.89				13	yes, no
	log(TP)		0.46				13	no
DelSontro et al. 2016	Sediment temp (ponds)	0.59					77	yes
	Sediment temp (lakes)	0.015					83	no
	log(TP) + Sediment temp + log(TP)*Sediment temp	0.52					89	yes
Wik et al. 2016	Waterbody type					8.857	51	yes
	Sediment type					8.937		yes
	log(depth)					0.047		no
	waterbody type*sediment type					0.086		no
	waterbody type*log(depth)					8.491		no
	sediment type*log(depth)					5.238		no
	Waterbody type					0.532	51	no
	Sediment type					0.946		no
	log(area)					3.444		no
	waterbody type*sediment type					3.405		no
	waterbody type*log(area)					2.955		no
	sediment type*log(area)					0.444		no
DelSontro, Beaulieu, and Downing 2018	log(TP)	0.292		0.648			101	yes
	log(TN)	0.311		0.647			47	yes
	log(Chl a)	0.317		0.630			65	yes
	log(area)	0.013		0.775			137	no
	log(area)*log(TP)	0.292		0.648			101	yes
	log(area)*log(TN)	0.387		0.610			47	yes
	log(area)*log(chl a)	0.280		0.634			64	yes
Sanches et al. 2019	Estimation method						78	yes
	Climatic zone							yes
	Min temp							no
	Avg. temp							no
	Estimation method*max temp							no
	Estimation method*avg temp							no

	Climatic zone*max temp Climatic zone*avg temp Climatic zone*year Precipitation Climatic zone*min precip Min temp*avg temp Min temp*min precip Max temp*avg temp							no no no no no no no yes
	Area Landscape Min temp Avg temp Area*landscape	0.98					46	no yes yes yes yes
	Max precip Avg temp Year precip*DOC	0.91					19	no yes no
Kuhn et al. 2021	DOC	0.14			12.25	72	yes	
	Area	0.08			13.88	165	yes	
	Latitude	0.03			5.38	161	no	
	Water temp	0.06			5.55	68	no	
	Depth				0.02	152	no	
	Area	0.21			19.85	69	yes	
Deemer and Holgerson, 2021	Water temp	0.09				134	yes	
	Latitude	0.04				218	yes	
	In(Area)	0.00				216	no	
	In(Max depth)	0.07				135	yes	
	In(Mean depth)	0.00				87	no	
	In(DOC)	0.00				85	no	
	In(Chl a)	0.18				143	yes	
	Waterbody type + latitude + chl a + area	0.29		481.69		130		
	Waterbody type*chl a + latitude + area	0.29		483.17		130		

Table SI2. All compiled environmental variables with sources, variable descriptions, shorthand variable names, data formats, and spatial resolutions. Selected representative variables which appear in Tables 1-3 of the main text are shown in bold. Representative variable selection was based on the highest adj. R² and lowest AIC within each dataset, except in the cases of the climate (Thornton et al. 2020) and soil carbon (Poggio et al. 2021) datasets, where variables were so highly correlated (Figures SI4 and SI5) that physical meaningfulness of the variables was also taken into account.

Source	Variable Description	Variable Name	Data Format	Resolution	n	
Engram, Walter Anthony, and Meyer 2020	Region (Atqasuk, Barrow, Fairbanks, Seward, or Toolik)	Region	Categorical	0.005 km ²	5,143	
	Methane ebullition flux (mg m ⁻² d ⁻¹)	MassFlxCH4	Vector	0.005 km ²		
	Lake area (km ²)	AreaSkm				
Derived from Engram, Walter Anthony, and Meyer 2020	Lake perimeter (km)	perimeter	Tabular	0.005 km ²		
	Buffer ratio	bf_pr_wi				
	Perimeter-to-area (P/A) ratio	p_a_ratio				
Messager et al. 2016	Shoreline development	Shore_dev	Vector	0.1 km ²	1,224	
	Lake volume (mcm)	Vol_total				
	Lake depth (m)	Depth_avg				
	Watershed area (km ²)	Wshd_area				
Pastick et al. 2015	Mean permafrost probability within 1 m of the surface	Pfrst_mean	Raster	30 m	5,143	
Wang et al. 2019	Fraction of combined wetland class (LWF) in lake and surrounding wetlands within 100m of lake	Ibf_100n	Raster	30 m	5,139	
	Fraction of littoral zone in lake and surrounding wetlands within 100m of lake	littoral_100n				
	Fraction of bog in lake and surrounding wetlands within 100m of lake	bog_100n				
	Fraction of fen in lake and surrounding wetlands within 100m of lake	fen_100n				
	Fraction of sparsely vegetated land among land pixels within 100m of lake	sparseveg_100n				
	Fraction of deciduous forest among land pixels within 100m of lake	decid_100n				

	Fraction of evergreen forest among land pixels within 100m of lake	evrgrn_100n			
	Fraction of barren land among land pixels within 100m of lake	barren_100n			
	Fraction of shrubland among land pixels within 100m of lake	shrub_100n			
	Fraction of herbaceous land among land pixels within 100m of lake	herb_100n			
Thornton et al. 2020	Average winter temperature (°C)	Tavg_W	Raster	1 km	5,141
	Average annual temperature (°C)	Tavg_yr			
	Average annual vapor pressure (Pa)	Vpavg_yr			
	Maximum annual temperature (°C)	Tmax_yr			
	Minimum annual temperature (°C)	Tmin_yr			
	Total annual precipitation (mm)	Precip_yr			
Poggio et al. 2021	Organic carbon stocks (t/ha)	SOCS	Raster	250 m	5,130
	Soil organic carbon content in the fine earth fraction (dg/kg)	SOC			
	Proportion of silt particles (≥ 0.002 mm and ≤ 0.05 mm) in the fine earth fraction (g/kg)	Silt			
	Proportion of sand particles (> 0.05 mm) in the fine earth fraction (g/kg)	Sand			
	Soil pH (pHx10)	Soil_pH			
	Organic carbon density (hg/m ³)	OCD			
	Total nitrogen (N) (cg/kg)	Nitrogen			
	Cation Exchange Capacity of the soil (mmol(c)/kg)	Cat_Ex			
	Bulk density of the fine earth fraction (cg/cm ³)	Bulk_Dens			
	Proportion of clay particles (< 0.002 mm) in the fine earth fraction (g/kg)	Clay			
	Volumetric fraction of coarse fragments (> 2 mm) (cm ³ /dm ³ (vol%))	Co_Frag			
Kuhn and Butman, 2021	Mean Landsat growing season surface reflectance (Rs) in the green wavelengths	Greenness	Tabular	0.1 km ²	1,061

Table SI3. Individual regression results for all assembled variables sorted and shaded by dataset (colors indicate divisions between datasets). Selected representative variables which appear in Tables 1-3 of the main text are shown in bold. Representative variable selection was based on the highest adj. R² and lowest AIC within each dataset, except in the cases of the climate (Thornton et al. 2020) and soil carbon (Poggio et al. 2021) datasets, where variables were so highly correlated (Figures SI4 and SI5) that physical meaningfulness of the variables was also taken into account.

Variable	rs	r2_adj	aic	n	cond_no	p < 0.005
Region	0.321	0.320	3845	5143	5.99	yes
AreaSqkm	0.201	0.201	4678	5143	5.47	yes
perimeter	0.176	0.176	4836	5143	30.1	yes
bf_per_wi	0.166	0.166	4895	5143	36.6	yes
p_a_ratio	0.175	0.175	4838	5143	11.8	yes
Shore_dev	0.002	0.001	873.2	1224	8.68	no
Vol_total	0.009	0.008	864.5	1224	2.23	yes
Depth_avg	0.026	0.026	842.9	1224	7.27	no
Wshd_area	0.003	0.003	871.6	1224	1.42	no
Pfrst_mean	0.038	0.038	5630	5143	32.3	yes
Ibf_100n	0.211	0.211	4564	5132	8.49	yes
barren_100n	0.007	0.006	5794	5139	33.6	yes
bog_100n	0.000	0.000	5826	5139	2760	no
decid_100n	0.028	0.027	5684	5139	92.9	yes
evrgrn_100n	0.000	0.000	5826	5139	24.0	no
fen_100n	0.030	0.030	5672	5139	38.1	yes
herb_100n	0.073	0.073	5438	5139	14.8	yes
littoral_100n	0.112	0.112	5173	5132	13.9	yes
shrub_100n	0.099	0.099	4964	5017	10.4	yes
sparseveg_100n	0.163	0.163	4915	5139	11.2	yes
Tavg_W	0.157	0.157	4949	5141	2670	yes
Tavg_yr	0.147	0.147	5011	5141	2690	yes

VPavg_yr	0.160	0.160	4934	5141	138	yes
Tmax_yr	0.046	0.046	5586	5141	2340	yes
Tmin_yr	0.043	0.042	5606	5141	6040	yes
Precip_yr	0.132	0.132	5103	5141	39.1	yes
SOCS	0.023	0.023	5679	5129	16.2	yes
SOC	0.060	0.059	5485	5129	42.2	yes
Silt	0.140	0.140	5028	5129	23.1	yes
Sand	0.010	0.010	5747	5129	24.4	yes
Soil_pH	0.075	0.075	5399	5129	14.2	yes
OCD	0.080	0.080	5370	5129	28.7	yes
Nitrogen	0.093	0.093	5297	5129	32.8	yes
Cat_Ex	0.071	0.071	5422	5129	26.4	yes
Bulk_Dens	0.116	0.116	5167	5129	12.3	yes
Clay	0.052	0.052	5527	5129	20.7	yes
Co_Frag	0.097	0.097	5278	5129	7.18	yes
Greenness	0.017	0.016	574.4	1061	28.2	yes

1. Supplementary Figures

Figure SI1. Correlation matrix for lake morphometry variables derived from Engram, Walter Anthony, and Meyer (2020).

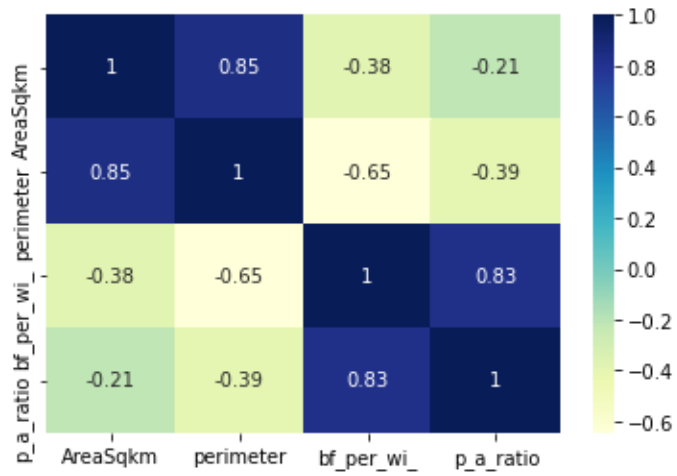


Figure SI2. Correlation matrix for lake morphometry variables from Messager et al. (2016).

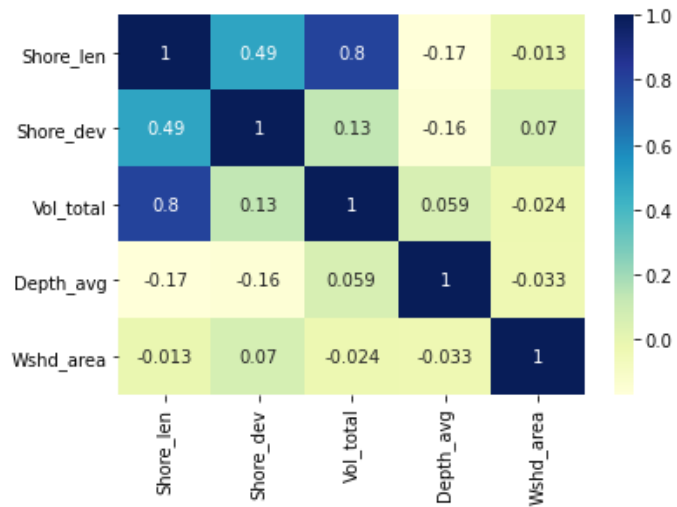


Figure SI3. Correlation matrix for land cover variables from Wang et al. (2020).

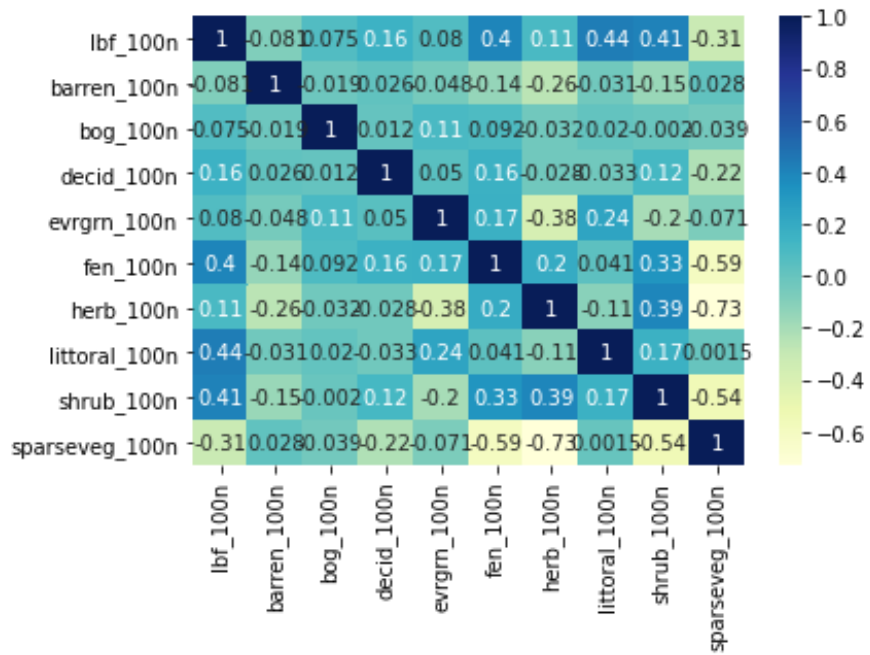


Figure SI4. Correlation matrix for climate variables from Thornton et al. (2020).

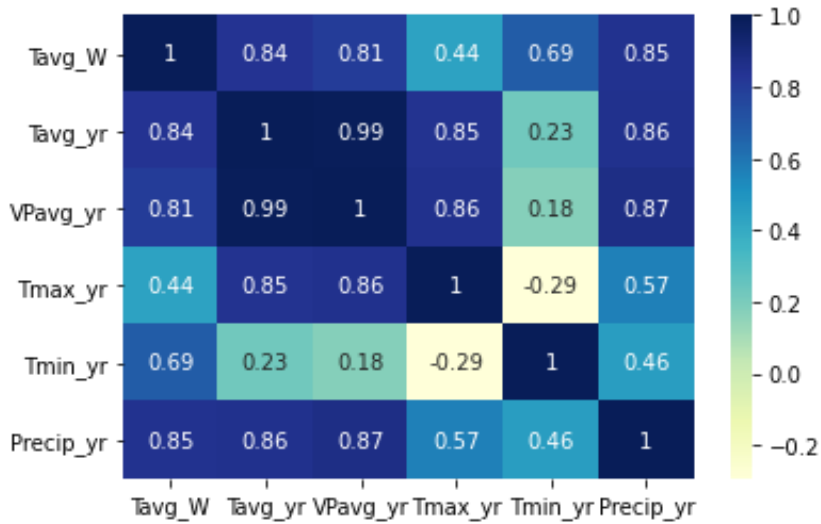


Figure SI5. Correlation matrix for soil variables from Poggio et al. (2021).

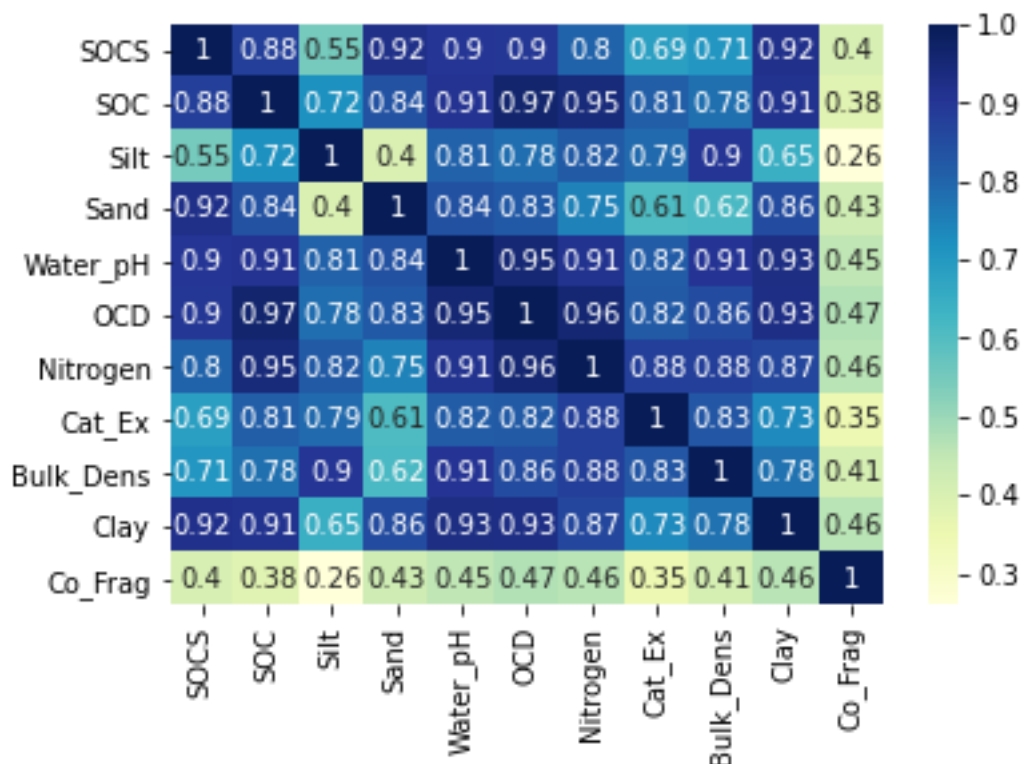
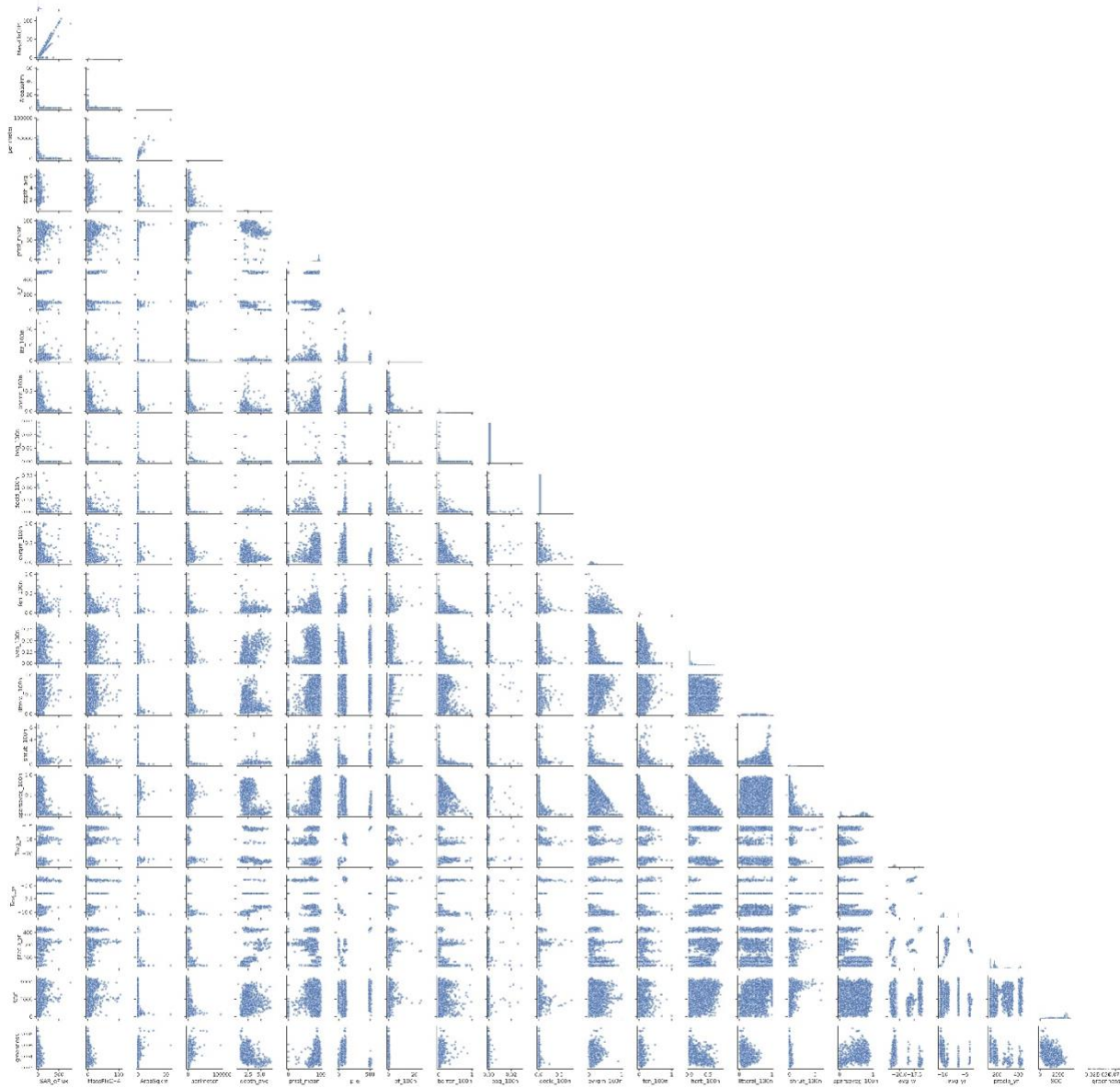


Figure SI6. Pair plots of volumetric and mass-based ebullitive methane fluxes for selected predictor variables. Histograms are shown on the diagonal elements and scatter plots on the lower diagonal elements. Figure is high-resolution and can be zoomed to view individual plots.



3. References

- Bastviken, D., J. Cole, M. Pace, and L. Tranvik. 2004. Methane emissions from lakes: Dependence of lake characteristics, two regional assessments, and a global estimate. *Global biogeochemical cycles*, 18(4). doi: 10.1029/2004gb002238.
- Deemer, B.R. and M.A. Holgerson. 2021. Drivers of methane flux differ between lakes and reservoirs, complicating global upscaling efforts. *Journal of Geophysical Research: Biogeosciences*, 126(4), p.e2019JG005600. doi: 10.1029/2019JG005600.
- DelSontro, T., J.J. Beaulieu, and J.A. Downing. 2018. Greenhouse gas emissions from lakes and impoundments: Upscaling in the face of global change. *Limnology and Oceanography Letters*, 3(3), pp.64-75. doi: 10.1002/lo2.10073.
- DelSontro, T., L. Boutet, A. St-Pierre, P.A. del Giorgio, and Y.T. Prairie. 2016. Methane ebullition and diffusion from northern ponds and lakes regulated by the interaction between temperature and system productivity. *Limnology and Oceanography*, 61(S1), pp.S62-S77. doi: 10.1002/lno.10335.
- Engram, M.J., K. Walter Anthony, and F.J. Meyer. 2020. ABoVE: SAR-based Methane Ebullition Flux from Lakes, Five Regions, Alaska, 2007-2010. ORNL DAAC, Oak Ridge, Tennessee, USA. doi: 10.3334/ORNLDaac/1790.
- Kuhn, C., and D. Butman. 2021. ABoVE: Lake Growing Season Green Surface Reflectance Trends, AK and Canada, 1984-2019. ORNL DAAC, Oak Ridge, Tennessee, USA. doi: 0.3334/ORNLDaac/1866.
- Kuhn, M.A., R.K. Varner, D. Bastviken, P. Crill, S. MacIntyre, M. Turetsky, K. Walter Anthony, A.D. McGuire, and D. Olefeldt. 2021. BAWLD-CH 4: a comprehensive dataset of methane fluxes from boreal and arctic ecosystems. *Earth System Science Data*, 13(11), pp.5151-5189. doi: 10.5194/essd-13-5151-2021.

Messager, M.L., B. Lehner, G. Grill, I. Nedeva, and O. Schmitt. 2016. Estimating the volume and age of water stored in global lakes using a geo-statistical approach. *Nature communications*, 7(1), pp.1-11. doi: 10.1038/ncomms13603. Data is available at www.hydrosheads.org.

Pastick, N.J., M.T. Jorgenson, B.K. Wylie, S.J. Nield, K.D. Johnson, and A.O. Finley. 2015. Distribution of near-surface permafrost in Alaska: Estimates of present and future conditions. *Remote Sensing of Environment*, 168, pp.301-315. doi: 10.1016/j.rse.2015.07.019.

Poggio, L., L.M. De Sousa, N.H. Batjes, G. Heuvelink, B. Kempen, E. Ribeiro, and D. Rossiter. 2021. SoilGrids 2.0: producing soil information for the globe with quantified spatial uncertainty. *Soil*, 7(1), pp.217-240. doi: 10.5194/soil-7-217-2021.

Sanches, L.F., B. Guenet, C.C. Marinho, N. Barros, and F. de Assis Esteves. 2019. Global regulation of methane emission from natural lakes. *Scientific Reports*, 9(1), pp.1-10. doi: 10.1038/s41598-018-36519-5.

Thornton, M.M., R. Shrestha, Y. Wei, P.E. Thornton, S. Kao, and B.E. Wilson. 2020. Daymet: Daily Surface Weather Data on a 1-km Grid for North America, Version 4. ORNL DAAC, Oak Ridge, Tennessee, USA. doi: 10.3334/ORNLDAA/1840.

Wang, J.A., D. Sulla-Menashe, C.E. Woodcock, O. Sonnentag, R.F. Keeling, and M.A. Friedl. 2019. ABoVE: Landsat-derived Annual Dominant Land Cover Across ABoVE Core Domain, 1984-2014. ORNL DAAC, Oak Ridge, Tennessee, USA. doi: 10.3334/ORNLDAA/1691.

Wik, M., R.K. Varner, K.W. Anthony, S. MacIntyre, and D. Bastviken. 2016. Climate-sensitive northern lakes and ponds are critical components of methane release. *Nature Geoscience*, 9(2), pp.99-105. doi: 10.1038/ngeo2578.